A&A 379, 46–53 (2001)
DOI: 10.1051/0004-6361:20011182

Astronomy & Astrophysics

*Beppo*SAX view of NGC 526A: A Seyfert 1.9 galaxy with a flat spectrum

R. Landi[1,2], L. Bassani[2], G. Malaguti[2], M. Cappi[2], A. Comastri[3], M. Dadina[1], G. Di Cocco[2], A. C. Fabian[4], E. Palazzi[2], G. G. C. Palumbo[5], and M. Trifoglio[1]

[1] Dipartimento di Fisica, Università di Bologna, via Irnerio 46, 40127 Bologna, Italy
[2] ITeSRE/CNR, via Piero Gobetti 101, 40129 Bologna, Italy
[3] Osservatorio Astronomico di Bologna, via Ranzani 1, 40127 Bologna, Italy
[4] Institute of Astronomy, Madingley Road, Cambridge CB3 0HA, UK
[5] Dipartimento di Astronomia, Università di Bologna, via Ranzani 1, 40127 Bologna, Italy

Received 11 April 2001 / Accepted 6 August 2001

Abstract. In the present work we report the *Beppo*SAX observation of the Seyfert 1.9 galaxy NGC 526A in the band 0.1–150 keV. The high energy instrument onboard, PDS, has succeeded in measuring for the first time the spectrum of this source in the 13–150 keV range. The combined analysis of all Narrow Field Instruments provides a power law spectral index of $\simeq$1.6 and confirms the flat spectral nature of this source. Although NGC 526A varies strongly in the 2–10 keV range over a period of months/years, its spectral shape remains constant over these timescales. An $Fe_{K\alpha}$ line, characterized by a complex structure, has been detected in the 6–7 keV range. The line, which has an equivalent width of 120 eV, is not compatible with being produced in an absorbing medium with $N_H \sim 10^{22}$ cm^{-2}, but most likely originates by reflection in an accretion disk viewed at an intermediate inclination angle of $\sim$42°. The reflection component is however small ($R \leq 0.7$) and so it is not sufficient to steepen the spectrum to photon index values more typical of AGNs. Instead, we find that the data are more consistent with a flat power law spectrum cut–off at around 100 keV plus a small reflection component which could explain the observed iron line. Thus NGC 526A is the only bona–fide Seyfert 2 galaxy which maintains a "flat spectrum" even when broad band data are considered: in this sense its properties, with respect to the general class of Seyfert 2's, are analogous to those of NGC 4151 with respect to the vast majority of Seyfert 1's.

Key words. X–rays: galaxies – galaxies: Seyfert – galaxies: individual: NGC 526A

1. Introduction

NGC 526A, a prototype Narrow Emission Line Galaxy (NELG), is a relatively nearby ($z = 0.0192$) S0 peculiar type galaxy which is the brightest member of a strongly interacting pair. Although the source is often classified as a Seyfert 1–1.5 in various databases (see NED and Simbad), it is a true example of a type 1.9 Seyfert. In fact in the NGC 526A discovery paper (Griffiths et al. 1979), it was stated that a broad component was only visible for Hα. This was subsequently confirmed by Winkler (1992) who also reports lack of any broad Hβ component during a more intense state of the broad Hα line. The low value of the narrow Hα/Hβ ratio (=3.0) indicates that the narrow line region is essentially unreddened, while the broad line region suffers significant obscuration as the broad Hα/H$\beta \geq 10$.

The galaxy, first identified as an X–ray source by the *HEAO–1*/SMC experiment (Griffiths et al. 1979), is one of the brightest extragalactic objects, being one of the Piccinotti sample sources. As such it has been the target of various X–ray observations in both soft and hard X–rays since its discovery (see Polletta et al. 1996 for a recent compendium of X–ray data).

At soft energies, *ROSAT* data are compatible with the source being point–like and having a 0.1–2.4 keV flux of 0.2×10^{-11} erg cm^{-2} s^{-1} (Rush et al. 1996). The source is strongly variable in the 2–10 keV band by a factor of $\sim$5. The spectrum in this band is fairly simple, being characterized by an absorbed ($N_H \sim 2 \times 10^{22}$ cm^{-2}) power law with a photon index of 1.5–1.6 (Smith & Done 1996; Turner et al. 1997): since in NGC 526A the spectrum remains flat, notwithstanding the use of more complex models, the source has been taken as a prototype of the "flat spectrum" Seyfert 2.

This flat shape is incompatible with current theories of Seyfert unification schemes, which predict steeper intrinsic

Send offprint requests to: R. Landi,
e-mail: landi@tesre.bo.cnr.it

power law of $\Gamma = 1.8$–2.0 as generally observed in Seyfert 1 galaxies. However, discrepancies from these schemes have been reported for Seyfert 2 galaxies in the sense that both flatter and steeper power law indices have been observed (Smith & Done 1996; Awaki et al. 1991). In a few cases the observations have been reconciled with the Unification Scenario by introducing complex absorption in the source and/or reflection (Cappi et al. 1996; Vignali et al. 1998; Malizia et al. 1999; Lanzi 2000; Malaguti et al. 1999). Furthermore, recent work using *OSSE* data alone or combined with low energy data, indicates that the average intrinsic spectrum of Seyfert 2 galaxies may be substantially harder than that of Seyfert 1, again in contrast with unified models of AGN (Zdziarski et al. 2000 and references therein). Thus the problem of "flat spectrum" Seyfert 2 galaxies is still an open issue, particularly for the relevance it may have with respect to the synthesis of the X–ray background.

The X–ray spectrum of NGC 526A is also characterized by a strong $Fe_{K\alpha}$ line, most likely due to an accretion disk: the data can be modeled equally well with the superposition of a component from an accretion disk viewed at 34° (Weaver & Reynolds 1985) plus a torus contribution or with a single feature from a nearly pole–on accretion disk (Turner et al. 1998). The observation of this line feature is in contrast with the lack of a strong reflection component: *Ginga* data put an upper limit to R (the strength of the reflected signal relative to the level of the incident radiation) at 0.5 (Smith & Done 1996).

NGC 526A has also been observed at high energies both by *OSSE* and *BATSE* on the *CGRO*: the 20–100 keV flux was observed to be in the range $(8$–$12) \times 10^{-11}$ erg cm^{-2} s^{-1} (Malizia et al. 1999; Zdziarski et al. 2000). Here we present the broad band (0.1–150 keV) spectrum of NGC 526A obtained by *Beppo*SAX NFI, which defines the source spectral components and consequently solves some of the still open questions regarding this object. In particular, we demonstrate that the source spectrum is indeed flat as previously suggested and has an exponential cut–off at around 100 keV.

2. Observation and data reduction

The *Beppo*SAX X–ray observatory (Boella et al. 1997) is a major programme of the Italian Space Agency with participation of the Netherlands Agency for Aereospace Programs.

This work concerns results obtained with three of the Narrow Field Instruments (NFI) onboard: the Low Energy Concentrator Spectrometer (LECS; Parmar et al. 1997), the Medium Energy Concentrator Spectrometers (MECS; Boella et al. 1997) and the Phoswich Detector System (PDS; Frontera et al. 1997).

*Beppo*SAX NFI pointed at NGC 526A from Dec. 31th 1998, to Jan. 2th 1999. The effective exposure times were 3.83×10^4 s for the LECS, 9.32×10^4 s for the MECS and 4.64×10^4 s for the PDS.

The data reduction and analysis have been performed using FTOOLS 4.1 and XANADU 10.0 software packages using standard techniques and selection criteria.

Another source (named SAX J0122.8–3448) has been detected in the MECS field of view at position $\alpha(2000) = 01^{\rm h}22^{\rm m}47.5^{\rm s}$, $\delta(2000) = -34°48'22''$, with an uncertain circle of $1'$ in radius (more details in the Appendix).

Apart from NGC 526A and the new MECS detection, no other known sources emitting in the 2–150 band are known to be present in the PDS field of view of 1.3 degrees (*FWHM*). Due to the large difference in flux, it is unlikely that this new MECS source contaminates the high energy emission of NGC 526A.

Light curves and spectra were extracted from a region centered in NGC 526A with a radius of $4'$ and $8'$ for the MECS and the LECS respectively. The source plus background light curves of each NFI did not indicate any significant variability; therefore, the data were integrated over the entire observing period to obtain an average spectrum of the source. LECS and MECS background subtraction was performed by means of blank sky deep field exposures accumulated by the *Beppo*SAX Science Data Center in the first year of the mission.

The PDS reduction was performed using the XAS software package and taking into account both rise time and spike corrections; products were obtained by plain subtraction of the "OFF" from the "ON" source data.

No HPGSPC data will be considered in the present paper as the source is too faint for a correct background subtraction.

3. Spectral analysis

LECS and MECS data were rebinned in order to sample the energy resolution of the detector with an accuracy proportional to the count rate: two channels for the LECS and four channels for the MECS. The PDS data were instead rebinned so as to have logarithmically equal energy intervals. The data rebinning is also required to have at least 20 counts per channel to ensure applicability of the χ^2 statistics. Spectral data from LECS, MECS and PDS data have been fitted simultaneously. We restricted the spectral analysis to 0.1–4.0 keV and 1.8–10.5 keV energy bands for the LECS and MECS respectively as these are the energy ranges where the response matrices released in September 1997 are best calibrated. The PDS analysis was restricted to data below 150 keV as the source signal disappears above this energy.

Normalization constants have been introduced to allow for known differences in the absolute cross–calibration between the detectors.

The values of the two constants have been allowed to vary. Using the absorbed power law model the LECS/MECS and PDS/MECS constants turned out to be 0.62 ± 0.04 and 0.82 ± 0.13 respectively. In all other models both constants have been constrain to lie within the suggested intervals (Fiore et al. 1999).

The spectral analysis has been performed by means of the XSPEC 10.0 package, and using the instrument response matrices released by the *Beppo*SAX Science Data Centre in September 1997.

All the quoted errors correspond to 90% confidence intervals for one interesting parameter ($\Delta\chi^2 = 2.71$). All the models used in what follows, contain an additional term to allow for the absorption of X–rays due to our galaxy, which in the direction of NGC 526A is caused by a column density of 2.2×10^{20} cm^{-2}.

During the *Beppo*SAX observation, NGC 526A was at a 2–10 (20–100) keV flux level of 1.8 (2.4) $\times$ 10^{-11} erg cm^{-2} s^{-1}, i.e. almost a factor of 2 (3–5) dimmer than when observed by *ASCA (BATSE/OSSE)* (Turner et al. 1997; Malizia et al. 1999; Zdziarski et al. 2000) but 60–70% brighter than when measured by *Ginga* (Smith & Done 1996).

3.1. The 0.1–10.5 keV spectrum

To check consistency with previous X–ray data, we first concentrated on the 0.1–10 keV band and fit the LECS–MECS spectrum with a simple absorbed power law model. The fit is not satisfactory ($\chi^2/\nu = 156/107$), as a soft excess and a line feature around 6–7 keV are evident in the model to data ratio (Fig. 1), and results in a flat spectrum having a photon index $\Gamma = 1.45 \pm 0.05$, absorbed by a column density of $N_{\rm H} = (1.33 \pm 0.15) \times 10^{22}$ cm^{-2}.

The photon index is significantly lower than the canonical value generally found in Seyfert galaxies, confirming the flat spectral nature of NGC 526A reported by *Ginga* and *ASCA* (Smith & Done 1996; Turner et al. 1997); note that this flat spectrum is found at different flux values, indicating that it is not a result of spectral variability. The absorbing column is consistent with previous measurements which implies that the state of the absorber is not effected by the state of the source.

In order to improve the quality of the fit, we fitted the data by adding to the previous model a narrow ($\sigma = 0$ keV) Gaussian line to account for excess emission around 6–7 keV. The line feature is centered at $6.52^{+0.13}_{-0.16}$ keV and has an equivalent width $EW = 121^{+47}_{-44}$ eV.

If the line width is allowed to vary, the additional parameter gives a statistical improvement in the fit ($\Delta\chi^2 = 2.6$ for one additional parameter) and the width observed is $0.28^{+0.21}_{-0.16}$ keV. However, from the confidence contours of the line against the energy, we conclude that the width is consistent with zero and quote a 90% upper limit of 0.6 keV. Similar values for the line parameters were also found by *Ginga* and *ASCA*.

Due to the low statistics available below 2 keV, no deep investigation is possible of the soft excess. We have tried to fit it with the following models: (a) power law, (b) partial covering power law with photon index equal to the one characterizing the primary continuum and (c) Raymond–Smith plasma.

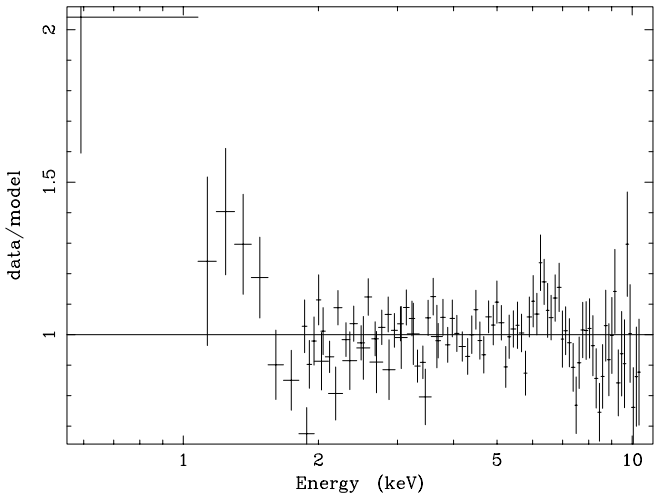

Fig. 1. Data to model ratio obtained from fitting the LECS and MECS spectra with a simple absorbed power law.

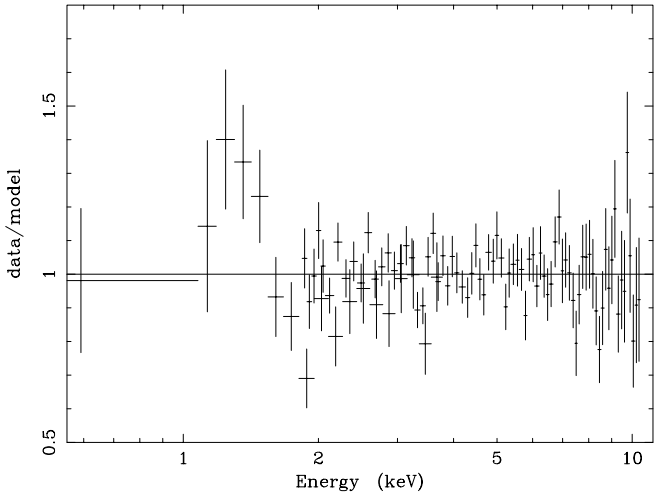

Fig. 2. Data to model ratio obtained from fitting the LECS and MECS spectra with a power law, to account for the soft excess, and an absorbed power law plus a Gaussian narrow line to describe the high energy data.

In each case, only galactic absorption was assumed for this component. Each model provides a significant improvement in the quality of the fit (>99%) and results in a photon index of $1.64^{+1.30}_{-0.75}$ for model (a), a column density of $(0.97^{+6.50}_{-0.42}) \times 10^{22}$ cm^{-2} with a covering fraction of $0.97^{+0.03}_{-0.10}$ for model (b) and a temperature of $0.17^{+0.14}_{-0.06}$ keV for model (c). The ratio/data model for case (a) is shown in Fig. 2.

In all cases the 0.1–2.4 keV flux is 0.16×10^{-11} erg cm^{-2} s^{-1} in agreement with *ROSAT* measurement. Despite the improvement in the quality of the fit, a local wiggle still remains around 1–2 keV in model (a) and (c) (see Fig. 2). This may be due to unresolved lines in this region or to an extra component (which requires absorption in excess of the galactic value) not accounted for in the fit.

Note that a similar soft X–ray spectral complexity of uncertain origin was also found by Turner et al. (1998) in

their analysis of the *ASCA* data. Unfortunately the statistics in the low energy band prevents us from making any definite statement on the nature of the soft excess. In any case the overall LECS–MECS data on NGC 526A confirm basically the previous results obtained by *Ginga* and *ASCA*, but allowing a spectral characterization during a different flux level: contrary to other Seyfert 2 galaxies, (Dadina et al. 2000; Turner et al. 1997) NGC 526A seems to have a stable spectral behaviour despite a significant change in the level of the continuum emission.

3.2. The PDS high-energy spectrum

The high energy spectrum (13–150 keV) measured by the PDS is well fitted ($\chi^2/\nu = 10.9/12$) by a simple power law model with $\Gamma = 1.79^{+0.18}_{-0.20}$.

In the effort of verifying and quantifying the significance of this spectral steepening above 10 keV, a broken power law (plus the narrow iron line) model was used to describe the MECS–PDS data (1.8–150 keV). For simplicity the knee of the broken power law was frozen at 10 keV, but a knee with free energy did not affected the results significantly. The model provides a good ($\chi^2/\nu = 89.5/84$) fit to the data and the following photon indices: $\Gamma_{2-10} = 1.56 \pm 0.07$ and $\Gamma_{13-150} = 1.78 \pm 0.2$.

It is still possible, however, for the source to have an intrinsically flat spectrum. The observed spectral steepening at $E > 13$ keV is then due to the exponential cut–off of the primary power law.

We have tested this model against our data and found that the fit ($\chi^2/\nu = 88.7/84$) is equally good (if not better) and gives a photon index: $\Gamma = 1.52 \pm 0.08$ with a cut–off value at 149^{+635}_{-74} keV.

We cannot therefore discriminate between this model and a broken power law one, but can only conclude at this stage that the PDS spectrum is steeper than the MECS one and look for other characterizations of the source to determine the real shape of the primary continuum.

3.3. The iron line

Although we do not find a broad line, inspection of Fig. 2 indicates that some residuals are still present around 7 keV. This combined with the slightly higher line energy measured (compared with the expected 6.4 keV) suggests the presence of a more complex line structure as also reported for the *ASCA* data (Turner et al. 1998; Weaver et al. 1985).

If the observed iron line is produced in the molecular torus (via transmission and/or reflection), we expect an $EW \leq 20$ eV for a column of $\sim 10^{22}$ cm^{-2} (Ghisellini et al. 1994); we therefore conclude that the observed line cannot be explained only by transmission in the absorbing material. Instead, the observed structure is reminiscent of a relativistic disk line profile (George & Fabian 1991).

In view of this indication, we have fitted the data using the *diskline* model in XSPEC (Fabian et al. 1989), assuming a Schwarzschild black hole having inner radius $R_{\rm in} = 6r_{\rm g}$, outer radius $R_{\rm out} = 1000r_{\rm g}$, (where $r_{\rm g} = MG/c^2$ is the gravitational radius and M is the mass of the black hole), and emissivity slope $\beta = -2.5$; furthermore, we fixed the line energy $E_{({\rm K}\alpha){\rm D}}$ at 6.4 keV, leaving as free parameters the disk inclination (i) and the line normalization.

In the following, the soft–excess is always parameterized with a scattering model (i.e. with a power law having the same photon index of the primary continuum) unless otherwise stated. The *diskline* model yields an improvement in the fit of $\Delta\chi^2 = 4.2$ (for an equal number of degrees of freedom) with respect to a narrow line model, and provides an inclination angle i and an $EW_{\rm D}$ in agreement with the *ASCA* results reported by Weaver et al. (1997) (see Table 1).

We have also tried to add a narrow line at 6.4 keV to the disk line component to account for the presence of a torus, but found no statistically significant improvement in the quality of the fit; in any case the torus component produces an $EW < 98$ eV.

Alternatively, the observed residual can be due to an extra narrow line at an energy $E_{({\rm K}\alpha)2} = 6.9$ keV (see Table 1): the fit is equally good ($\chi^2/\nu = 139.6/118$), if not better, but the origin of this extra line is more difficult to account for in a Compton thin source like NGC 526A.

Figure 2 also shows evidence for two possible edge structures in the 7–9 keV range: an edge at 7.4 having an optical depth of 0.45 was indeed reported by Turner et al. (1997).

We have tried to add such features in our spectrum but obtain no improvement in the fit. The upper limit we found for the optical depth is 0.16 for an edge at 7.1 keV, or 0.14 for an edge in the range 7.4–8.5 keV. These limits are compatible with column densities lower than 10^{23} cm^{-2}, i.e. there is no strong requirement for more absorption than observed.

However, in view of previous results on some flat spectra Seyfert 2 galaxies (Malaguti et al. 1999; Vignali et al. 1998), we have also tested our data against a complex absorber model. This can be parameterized by a dual absorber model, where two columns cover both uniformly the source (in this case the relative normalization gives the percentage of the source covered by each column), or by a partial plus uniform absorber model where one absorber covers only partially the source, while the other covers it totally. These two models are algebraically identical, but require slightly different assumptions on the source geometry (see Cappi 1998).

We have tested both models against our *Beppo*SAX broad data, and obtained a better fit ($\chi^2/\nu = 136.7/117$) for the first model. Note that in both cases no extra component is required to described the *soft–excess*, but if this is modeled with a scattering component, the results do not change significantly. The data indicate that 53% of the source is covered by a column of $\sim 10^{22}$ cm^{-2}, and 47% by a column of a few 10^{22} cm^{-2} (see Table 1).

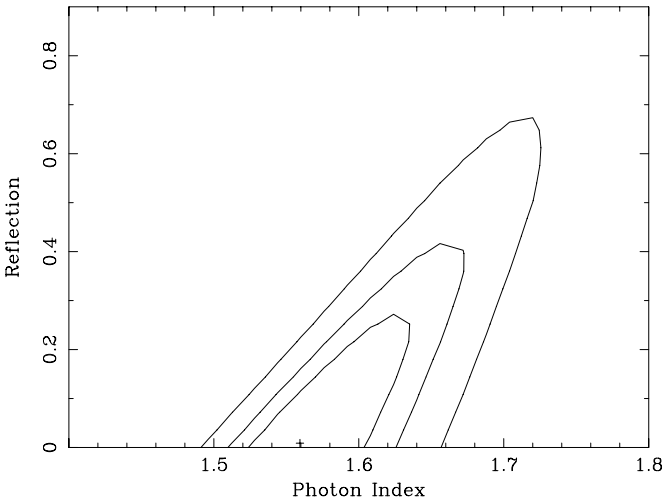

Fig. 3. Contour plot of the relative normalization between the primary and Compton reflected spectral components versus the intrinsic photon index.

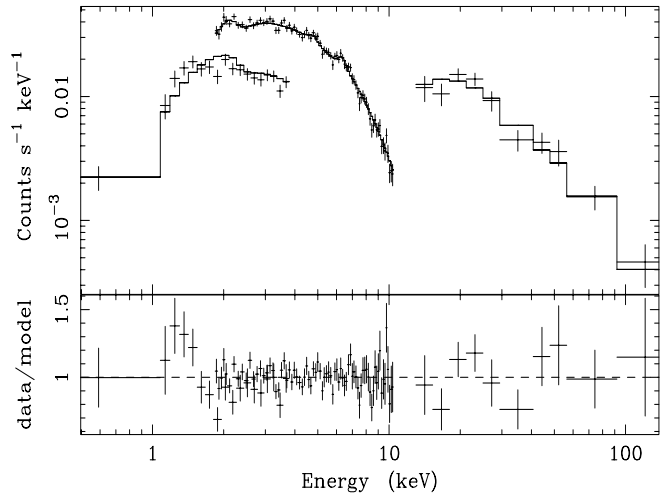

Fig. 4. MECS and PDS spectra best–fit model (*upper panel*) and data to model ratio (*lower panel*) for the PEXRAV model (in which the cut–off energy is allowed to vary) plus a narrow Gaussian line.

However, the spectrum remains flat since the data do not required a strong additional absorber. Also the column densities observed can only explain a line EW of $\sim$50 eV, much lower than the value reported for this model.

4. Defining the source spectral components

The previous analysis already gives a number of useful indications. First of all, the presence of complex absorption can not be used to explain the flat spectrum observed in the source, nor the line EW obtained by the data. Second, the line parameterization indicates the presence of a reflection component most likely due to an accretion disk.

We therefore conclude that reflection may play a role in this source and may be responsible for the flat spectrum observed.

Therefore, we have tried to fit the data with the PEXRAV model in XSPEC (Magdziarz & Zdziarski 1995), which consists of an exponentially cut–off power law reflected from a neutral slab, plus a narrow Gaussian line; all these components are absorbed by intrinsic absorption as expected in the case of reflection by an accretion disk.

Furthermore, we have fixed the disk inclination to 42° as estimated by the line spectral analysis. First, we assumed the cut–off to be high enough (10^4 keV) not to be effective in the fit: we obtain a photon index Γ of $\sim$1.6 and an upper limit to the reflection coefficient R (the solid angle in units of 2π subtended by the reflecting matter) of $\sim$0.3 (see Table 1). The contour plot of Γ versus R (Fig. 3) clearly shows that in any case the spectrum remains flat and incompatible with the canonical value of 1.9 even if the reflection is at the maximum value allowed by the fit (i.e. $R < 0.4$ at 90% confidence level). This strongly suggests that the data prefer a flat spectrum and a small reflection. If the cut–off energy is allowed to vary, we obtain a best fit model (Fig. 4) with a cut–off at an energy E_C

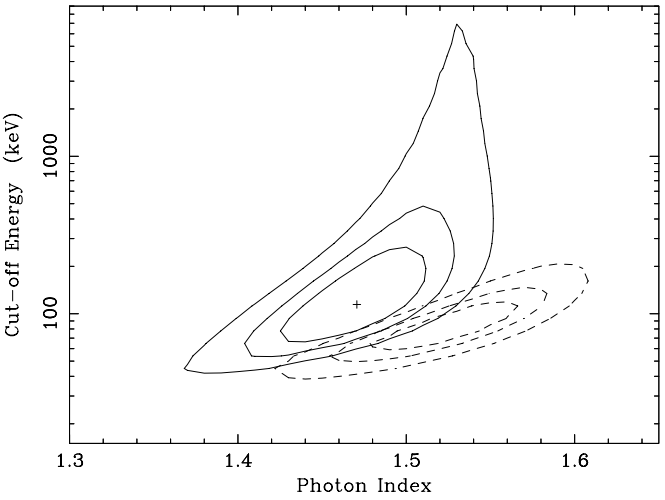

Fig. 5. Contour plot of the cut–off energy of the primary power law component versus the photon index for two possible reflection values: $R = 0$ (solid line) and $R = 0.7$ (dashed line).

at around 100 keV and $R < 0.7$ (see Table 1); in this case the improvement in the fit with respect to a pure power law is $\sim$95% or $\Delta\chi^2 = 7.2$ for two degrees of freedom.

Comparison with the previous model suggests that the data are more sensitive to the introduction of the cut–off energy rather than to the reflection component. In order to better define the cut-off energy, we have fixed the line parameters and the intrinsic absorption to their best values for two possible reflection value within the estimated range of uncertainty ($R = 0$ and $R = 0.7$): the contour plot of Γ versus cut–off energy for these cases is shown in Fig. 5 which clearly localize the power law exponential decline in the range 40–400 keV.

We have also tried an ionized reflection model, which provides a slightly higher reflection component ($R \sim 0.4$), an ionization parameter χ_i of $\sim$5 and a cut–off at around

Table 1. Principal models used to fit the data in the 0.1–150 keV band (see text).

Parameter	Double Gaussian line	diskline	Reflection $E_{\rm C} = 10^4$ keV	Reflection $E_{\rm C}$ free	Dual absorber
$N_{\rm H}$ (10^{22} cm^{-2})	$1.71^{+0.23}_{-0.17}$	$1.68^{+0.23}_{-0.18}$	$1.72^{+0.22}_{-0.27}$	$1.56^{+0.30}_{-0.20}$	$3.17^{+2.66}_{-1.32}$
$N_{\rm Hdabs}$ (10^{22} cm^{-2})	-	-	-	-	$0.96^{+0.27}_{-0.32}$
Γ	$1.56^{+0.07}_{-0.03}$	1.57 ± 0.04	$1.56^{+0.07}_{-0.04}$	$1.47^{+0.13}_{-0.07}$	1.65 ± 0.08
$E_{\rm K\alpha}$ (keV)	$6.4^{(f)}$	-	$6.53^{+0.17}_{-0.13}$	$6.52^{+0.20}_{-0.14}$	$6.54^{+0.20}_{-0.14}$
EW (eV)	103 ± 48	-	133 ± 47	121 ± 50	265 ± 100
$E_{\rm (K\alpha)2}$ (keV)	$6.9^{(f)}$	-	-	-	-
EW_2 (eV)	91^{+53}_{-51}	-	-	-	-
$E_{\rm (K\alpha)D}$ (keV)	-	$6.4^{(f)}$	-	-	-
$EW_{\rm D}$ (eV)	-	283^{+104}_{-94}	-	-	-
i (degrees)	-	$42.2^{+7.1}_{-9.7}$	-	-	-
$E_{\rm C}$ (keV)	-	-	$10^{4\,(f)}$	112^{+234}_{-50}	-
R	-	-	<0.3	<0.7	-
χ^2/ν	139.6/118	141.1/118	145/117	138.1/116	136.7/117

$^{(f)}$ The parameter is fixed at the value reported in the table.

140 keV ($\chi^2/\nu = 137.4/115$). However, even in this case the spectrum remains flat as the reflection is insufficient to steepen the high energy continuum.

Although the dual absorber model is statistically a slightly better fit with respect to the reflection model, it has more difficulties in explaining the iron line, both in terms of EW value and spectral profile.

In view of this, we assume as valid the reflection model and try, in the following, to verify the self–consistency of this assumption.

5. Discussion

The overall picture that emerges from the NGC 526A *Beppo*SAX data is that of a flat spectrum source absorbed by a column density of $\sim 10^{22}$ cm^{-2}. In the context of the reflection model, the source has a small reflection component ($R \leq 0.7$) and an iron line with an EW of 121 eV. The reflection component originates in an accretion disk seen at an angle of $\sim 42°$.

Recently Zdziarski et al. (1999) found a strong correlation between the amount of Compton reflection from neutral gas and the intrinsic spectral slope, in the sense that the reflection strength decreases with decreasing Γ. This correlation has a simple physical interpretation as long as the same medium that is responsible for the observed Compton reflection also plays a role in the cooling of the source hot plasma. Less reflection provides less cooling which in turn produces a flatter spectrum (Zdziarski et al. 1999). As the line is also produced in the same medium, a correlation between the strength of the reflection and the width of the $\rm Fe_{K\alpha}$ is also expected (Lubiński & Zdziarski 2000).

For a power law of index $\Gamma \sim 1.6$ and a viewing angle of 42° the expected relationship between EW and R is $EW \sim (140-160) \times R$ (George & Fabian 1991; Życky & Czerny 1994). In our case this yields an $EW < 100$ eV if $R < 0.7$, in agreement with the uncertainty range obtained with the reflection model, especially if part of the EW (at least 20 eV) is due to transmission in the absorbing medium and the reflecting medium is mildly ionized. Therefore, the line EW value and spectral profile are well

Table 2. Main characteristics of the sources found in the 2MASS Atlas Images.

Source	$\alpha(2000)$	$\delta(2000)$	$m_{\rm b}$	$m_{\rm r}$	J	H	K
1	$01^{\rm h}22^{\rm m}47.6^{\rm s}$	$-34^\circ48'46.6''$	18.4	17.1	16.165	15.543	14.650
2	$01^{\rm h}22^{\rm m}48.2^{\rm s}$	$-34^\circ48'57.3''$	20.1	17.9	16.345	15.400	15.088

described by a mildly ionized medium. Also our observation of a cut–off at around 100 keV (albeit the uncertainty range is large) agrees with the observed tendency for flat sources to avoid high values of the cut–off energy.

In a recent analysis of the cut–off versus power law index of a sample of Seyfert 1 galaxies observed with *Beppo*SAX, Matt (2000) finds that sources as flat as NGC 526A have a cut–off below 200 keV as indeed observed here. Although it is still debatable if this has a physical meaning or is due to a selection effect (i.e. it is more difficult to determine an high energy cut–off in steep sources), nevertheless our observation confirms this trend. The presence of a low energy cut–off also explains why the PDS data are steeper than the MECS ones.

Finally, this picture also explains the stable spectral shape observed in NGC 526A despite large changes in its flux level. If reflection is small at all flux levels, the power law component always dominates; therefore no spectral variations are observed as the source luminosity varies unless the primary power law shape changes.

On the basis of the above considerations, we are led to conclude that the overall picture is consistent with NGC 526A being an intrinsically flat spectrum source. On the other hand, NGC 526A is a bona–fide Seyfert 2 galaxy, as discussed in the introduction, and it is therefore a crucial object for testing the Unified Model. So far NGC 526A is the only Seyfert 2 confirmed as a flat spectrum source, the other objects reported have been found to be compatible with the "canonical" Seyfert spectral index of 1.8–2.0, when more complex models are considered.

In particular, analysis of *Beppo*SAX data of other sources from the Smith & Done sample, namely NGC 4507, NGC 2110 and MCG–5–23–16 (Lanzi 2000; Malaguti et al. 1999; Malizia et al. 2001) are all compatible with a canonical spectrum when analyzed over a broad band. Thus our observation suggests that flat Seyfert 2 galaxies exists but are not common. This finding does not necessarily contradict the Unified Models, since flat Seyfert 1 galaxies are also observed: Matt (2000) lists 3 such sources in his sample of Seyfert 1 galaxies, the most prominent being the atypical NGC 4151.

The X–ray continuum of Seyfert galaxies is commonly believed to be produced by Compton scattering of soft photons on a population of hot electrons. Assuming thermal equilibrium and a plane parallel geometry for the Comptonizing plasma above the accretion disk, the average properties of Seyfert galaxies could be naturally accounted for (Haardt & Maraschi 1991).

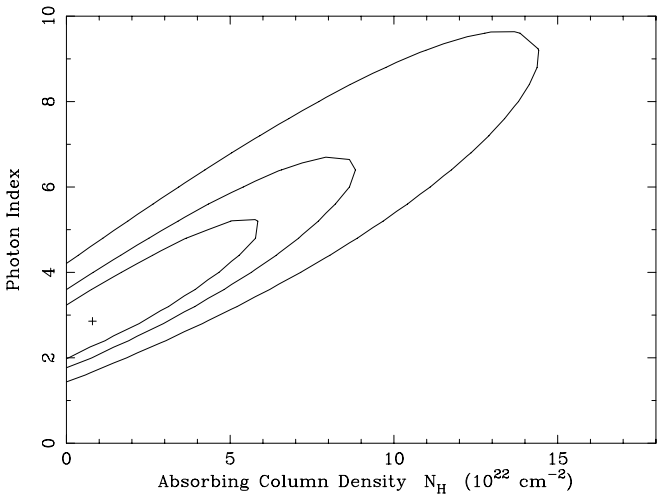

Fig. 6. Confidence contours for the photon index versus the equivalent Hydrogen column density in the absorbed power law model obtained for the source observed within the MECS field of view.

However, this model is unable to easily explain spectra flatter than $\Gamma \sim 2$. This has been traditionally the main concern about the existence of flat spectra source.

However Petrucci et al. (2000) have shown that the cut–off power law continuum + reflection usually employed to fit X–ray data is a too simple model as it derives a lower temperature and an higher optical depth for the hot plasma than obtained with accurate thermal Comptonization models, which treat carefully the anisotropy effects in Compton processes. In these models, the LECS and MECS data determine the slope below the anisotropy break. Above this break the intrinsic spectrum is steeper. It can thus fit the PDS data without an additional steepening beyond 100 keV. Within these models therefore flat spectra sources can be easily accounted for, thus removing the uncomfortable situation that they are "strange/peculiar" objects to our global understanding of Seyfert galaxies.

6. Appendix

In this section we briefly report some characteristics of the other source detected in the MECS field of view.

Within the MECS error box, we find a faint ROSAT source at position $\alpha(2000) = 01^{\rm h}22^{\rm m}50.3^{\rm s}$, $\delta(2000) = -34^\circ47'54''$ (37 arcsec positional uncertainty), having a

flux, in the 0.1–2.4 keV band, of $\sim 4 \times 10^{-13}$ erg cm^{-2} s^{-1}. Also in the MECS error box of $1'$, we find two sources from the MASS 2nd Incremental Release Point Source Catalogue, whose characteristics are shown in Table 2. The first object is identified with the galaxy APMUKS(BJ) B012030.16–350426.7. Neither of the 2 μm sources fall within the ROSAT error box.

Notwithstanding the low statistics of the data, we tried to analyze the MECS source spectrum extracted from a region centered in the source with a radius of $2'$.

First, we fitted the data with a simple power law: the model is satisfactory ($\chi^2 = 20.2/17$) and yields a photon index $\Gamma = 2.55^{+0.64}_{-0.77}$. The addition of intrinsic absorption to the previous model does not improve the quality of the fit ($\chi^2 = 20/16$) and gives a 90% upper limit of 6.5×10^{22} cm^{-2}. The confidence contours of the photon index against the absorbing column density are shown in Fig. 6.

The flux in the 2–10 keV band turned out to be 3.4×10^{-13} erg cm^{-2} s^{-1}.

Acknowledgements. This research has made use of SAXDAS linearized and cleaned event files produced at the *Beppo*SAX Science Data Centre. G.M., G.G.C.P., M.C. and L.B. acknowledge financial support from the Italian Space Agency. We would like to thank the referee Dr. H. Inoue for the very useful comments which have improved the quality of this work.

References

Awaki, H., Koyama, K., et al. 1991, PASJ, 43, 195
Boella, G., et al. 1997a, A&AS, 122, 299
Boella, G., et al. 1997b, A&AS, 122, 327
Cappi, M., et al. 1996, ApJ, 456, 141
Cappi, M. 1998, Ph.D. Thesis, University of Saitama
Fabian, A. C., et al. 1989, MNRAS, 238, 729
Fiore, F., Guainazzi, M., & Grandi, P. 1999, SAXabc, vs. 1.2, Cookbook for *Beppo*SAX NFI Spectral Analysis
Frontera, F., et al. 1997, A&AS, 122, 357
George, I. M., & Fabian, A. C. 1991, MNRAS, 249, 352
Ghisellini, G., et al. 1994, MNRAS, 267, 743
Griffiths, R. E., et al. 1979, ApJ, 230, L21
Lanzi, R. 2000, Master Thesis, University of Bologna
Lubiński, P., & Zdziarski, A. 2001, MNRAS, 323, L37
Magdziarz, P., & Zdziarski, A. A. 1995, MNRAS, 273, 837
Malaguti, G., et al. 1999, A&A, 342, L41
Malizia, A., Bassani, L., et al. 1999, ApJ, 519, 637
Malizia, A., et al. 2001, in preparation
Matt, G. 2001, ApJ, in press [astro-ph/0007105]
Parmar, A. N., et al. 1997, A&AS, 122, 309
Petrucci, P. O., et al. 2001, ApJ, in press [astro-ph/0004118]
Polletta, M., Bassani, L., et al. 1996, ApJS, 106, 399
Rush, B., et al. 1996, ApJ, 471, 190
Smith, D. A., & Done, C. 1996, MNRAS, 280, 355
Turner, T. J., George, I. M., Nandra, K., et al. 1997, ApJS, 113, 23
Turner, T. J., George, I. M., Nandra, K., et al. 1998, ApJ, 493, 91
Vignali, C., et al. 1998, A&A, 333, 411
Voges, W., et al. 2000, IAUC, 7432, 3
Weaver, K. A., & Reynolds, C. S. 1998, ApJ, 503, L39
Winkler, H. 1992, MNRAS, 257, 677
Zdziarski, A. A., Lubiński, P., & Smith, D. A. 1999, MNRAS, 303, L11
Zdziarski, A. A., et al. 2000, ApJ, 542, 703
Życki, P. T., & Czerny, B. 1994, MNRAS, 266, 653